

Modeling a heterogeneous metal/semiconductor interface: Ce on Si(111)

M. Grioni, J. Joyce, M. del Giudice, D. G. O'Neill, and J. H. Weaver

*Department of Chemical Engineering and Materials Science, University of Minnesota,
Minneapolis, Minnesota 55455*

(Received 20 September 1984)

High-resolution synchrotron radiation photoemission studies of Ce deposited onto cleaved Si(111)-2×1 reveal heterogeneous growth which involves clustering, Ce/Si reaction to form silicide patches, lateral silicide growth, and finally Ce overlayer formation with surface segregated Si. Core-level line-shape analysis reveals three distinct Si local bonding configurations. The relative interface concentration of each Si species has been determined as a function of overlayer thickness, and a model for this interface is presented and discussed.

Interface interactions are often modeled by uniform layers of reacted or unreacted material on stable substrates. Although the assumption of a homogeneous interface simplifies modeling,¹ it is not correct for many interfaces.²⁻¹⁶ Indeed, interface reactivity, kinetics, and chemical trapping are difficult to treat within the homogeneous layer model. Further, treatments of Schottky barrier formation based on uniform overlayers fall short of adequately describing the behavior of the barrier at low coverage.^{2,3} Unfortunately, while the importance of heterogeneity has long been recognized, few studies have been able to resolve lateral features at an interface.

In this Rapid Communication, we discuss an interface having a richness of phenomena related to heterogeneous growth: Ce/Si(111). As we will show, results obtained with high-resolution core-level photoemission make it possible to model even complicated systems by distinguishing the different electronic configurations of the constituents. Such core-level studies are complemented by valence-band results which emphasize changes in the states near the Fermi level E_F .

In a previous paper,¹⁷ we discussed the submonolayer behavior of the Ce/Si(111) interface, demonstrating cluster formation by combining core-level and valence-band photoemission, low-energy electron diffraction (LEED), and angle-resolved Auger spectroscopy. Here, we emphasize the development of the interface subsequent to the ripening of the clusters (reaction), describing the varying environments which evolve with coverage at room temperature.

The photoemission experiments were conducted at the Wisconsin Synchrotron Radiation Center using the Tantalus storage ring and the grasshopper and toroidal grating monochromators. The overall resolution of the measurements ranged from 200 meV at $h\nu=40$ eV to 500 meV at $h\nu=135$ eV. Ce was deposited onto cleaved Si(111)-2×1 surfaces in an experimental system described in detail elsewhere.¹⁸ During evaporation, the pressure rose from operating pressures of 3×10^{-11} to $\sim 1\times 10^{-10}$ Torr. Evaporation rates of ~ 1 Å/min and the use of a shutter permitted 0.04 ML incremental depositions without difficulty. In this paper, coverages will be defined in monolayers where 1 ML = 2.6 Å = 7.8×10^{14} atoms cm⁻², the surface density of Si.

In Fig. 1 we show valence-band energy distribution curves (EDC's) for Ce coverages 0-16 ML. Although the EDC's have been drawn with approximately the same height, comparison of absolute count rates shows that the Ce-derived

features very quickly dominate the Si emission, indicative of the higher photoionization cross section of Ce 5*d*4*f* states relative to Si *sp*³ states at $h\nu=40$ eV.¹⁹ The difference curve at the bottom of Fig. 1 gives the result of subtraction of normalized EDC's for clean Si and 0.4 ML Ce/Si. For this difference curve, the well-defined doublet 1.2 and 3.2 eV below E_F reveals emission from Ce-induced states and is indicative of weakly interacting Ce clusters, as proven by valence band, LEED, and angle-resolved Auger results.¹⁷ With increasing coverage, the spectral features change as peak "A" near E_F is lost and the valence band becomes relatively structureless. At that point, the interface photoemission spectra can no longer be described as the superposition of unreacted Si and Ce clusters. By $\theta=2.4$ ML the interface product is metallic with a distinct Fermi-level cutoff. At 4-ML coverage, a sharp feature emerges at E_F and grows relative to the deeper structure and the valence band narrows, ultimately converging to Ce. Figure 1, therefore, shows that valence-band emission can be readily identified at low coverage (clusters) and high coverage (Ce metal overlayer), but continuous evolution at intermediate coverage suggests a broad, intermixed interface or a heterogeneous interface. Core-level studies make it possible to rule out the former.

The results of Fig. 2 show the Si 2*p* core emission measured with high surface sensitivity [$h\nu=135$ eV, escape depth ~ 4 Å (Ref. 20)]. The bottom-most EDC for clean Si(111)-2×1 reveals the characteristic 2*p* doublet broadened by surface-shifted components.²⁰ At submonolayer coverage, it shifts rigidly to greater binding energy (band bending without chemical reaction).¹⁷ At $\theta\approx 0.6$ ML a reacted component appears and grows relative to the original component, as indicated by the tic marks shifted 0.67 eV. For $\theta\geq 3$ ML, a third Si doublet is observed at 1.2 eV lower binding energy than bulk Si. This component persists to very high coverage and the Si 2*p* line shape is significantly sharper than for the clean surface, suggesting a more atomic Si bonding configuration.

In Fig. 2, we also show the line-shape decomposition of the experimentally observed Si 2*p* emission into three spin-orbit-split pairs with branching ratios and spin-orbit splittings equal to those of Ref. 20. For each, the experimental full width at half maximum (FWHM) was derived from results at $\theta=0.2$ ML where the surface shifted component was small and the linewidth was a measure of our resolution. Comparison shows this FWHM to be ~ 0.1 eV larger than for the clean surface, analogous to what has been ob-

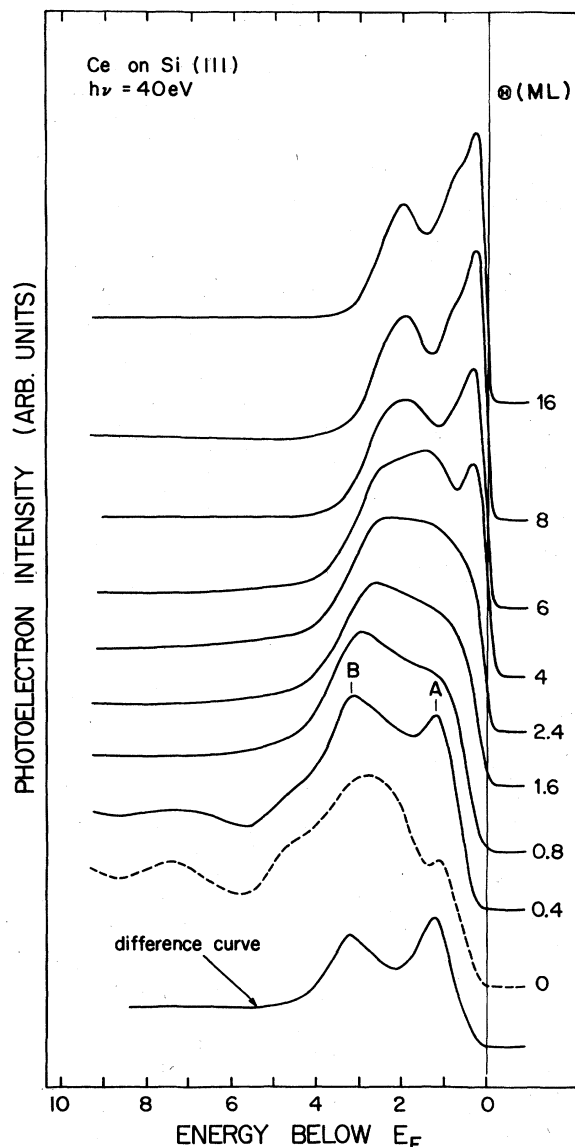


FIG. 1. Energy-distribution curves for Ce/Si showing valence-band evolution. The bottom-most curve represents the normalized difference between clean Si(111)- 2×1 and the interface with 0.4-ML coverage. At low coverage the spectra are superpositions of Ce and Si, at high coverage they converge to bulk Ce, but in the intermediate range, they reveal a heterogeneous interface.

served by Ludeke, Chiang, and Miller⁵ in detailed examinations of the nonreactive Ag/GaAs(110) interface. Such broadening is physically reasonable for the room-temperature reacted phase because of the likely existence of not-quite-identical bonding configurations for Si, i.e., to disorder within the dominant local bonding configuration. The significant conclusion from Fig. 2 is that the experimental line shapes can be fitted very well for all coverages by assuming only three unique Si configurations (three doublets).

The attenuation of the total Si $2p$ emission is a measure of the rate at which Si is masked by the overlayer. However, for a reacted interface with several components, it is much more informative to consider the attenuation of each

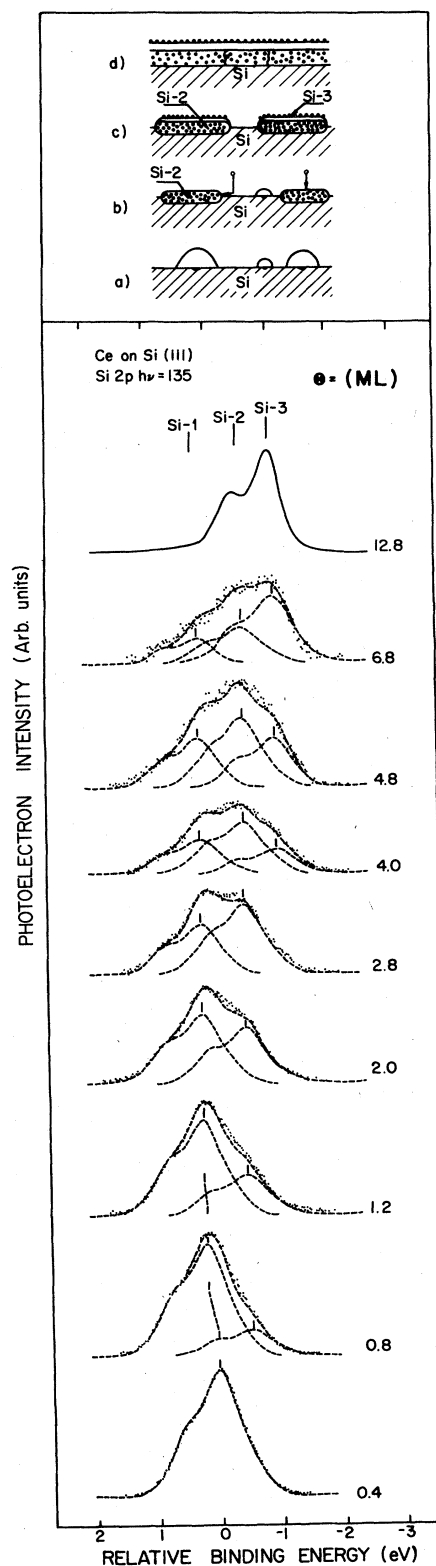


FIG. 2. EDC's on the left show the evolution of the Si $2p$ core emission. On the right, line-shape decompositions are shown for representative coverages. At any coverage, the results can be fitted with components representing clean Si (Si-1), a reacted phase (Si-2), and surface segregated Si (Si-3). Our model for the interface is shown pictorially on top of the figure.

component separately. In Fig. 3 we display the attenuation results for the three Si components,

$$\alpha_i = \ln[I(2p_i(\theta)/I(2p(\text{initial}))]$$

As shown, substrate Si-1 attenuation is rapid throughout the coverage range. The reacted Si-2 component grows with coverage from 0.6 to about 2.5 ML, but then diminishes sharply. The Si-3 component appears slightly above 3 ML and remains nearly constant with coverage, amounting to about 8% of the original Si intensity at $\theta = 24$ ML (not shown).

An interface with behavior demonstrated by Figs. 1–3 is complex, but the results presented here allow formulation of a model which describes its heterogeneous growth. Although clusters form below 0.6 ML, they interact weakly with the substrate and the Si 2*p* binding energy does not change. At 0.6 ML, conversion from cluster growth to reactive intermixing occurs. Nonetheless, upon reaction the disrupted surface area is still only a portion of the total surface, having resulted from intermixing beneath and adjacent to the clusters. The emergence of the Si-2 signal reveals Si in these patches and comparison with unreacted Si shows the chemical inequivalence of the two configurations.

At 0.6-ML coverage, where the reacted Si component is first observed, the featureless valence-band spectra give no evidence for a metallic Ce layer. However, both the valence bands and the core levels do indicate that a Ce layer forms shortly thereafter. In the valence bands, this can be seen by the reappearance near E_F of peak *A*—which ultimately becomes recognizable as Ce metal at high coverage. In the core levels, the fact that Si-2 reaches a maximum near 2.5 ML and is then rapidly attenuated indicates a covering up of the reacted species for $\theta \geq 2.5$ ML. Nonetheless, the rate of attenuation of this reacted Si-2 species is nearly exponential with a characteristic length of ~ 6 Å, i.e., an escape depth larger than expected for a uniform overlayer of an efficient scatterer like Ce.²¹ Likewise, the attenuation of the unreacted Si-1 species suggests the presence of uncovered Si substrate at relatively high coverage.

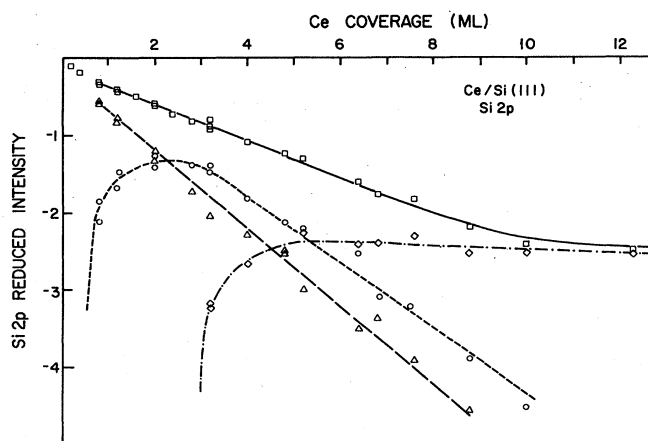


FIG. 3. Attenuation of the total Si 2*p* emission (solid line at top) and the attenuation of each of its three components. Although the substrate attenuation is rapid and monotonic, the reacted component grows to a maximum near 2.5 ML and is then attenuated. The surface-segregated component appears only after the reacted component is covered up by Ce and is nearly constant in magnitude to high coverage.

The results for the intermediate coverage regime can be reconciled by modeling the interface as a patchwork of reacted Si on a matrix of unreacted substrate. Ce deposited onto the clean matrix will have the high mobility of Ce observed at lowest coverage and can diffuse to the edge of the reacted patches. The perimeter of these patches provides active sites for continued reaction due to the disruption of the substrate covalent bonds. As a result, Ce silicide growth (i.e., conversion of Si-1 to Si-2) involves a portion of Ce adatoms in the coverage range 0.6–3 ML and the patches grow laterally. This continues until most of the surface is reacted at about 3-ML nominal coverage.

In the intermediate coverage range, Ce deposition onto the reacted patches must be treated differently from that onto the unreacted Si surface, as indicated by the behavior of the Si-2 species. The results of Figs. 1–3 indicate that, although the patches grow laterally, they apparently do not grow vertically. Instead, the reacted layer is rapidly covered up by Ce, as shown, for example, by the onset of the Ce-like valence-band features and the decay of the Si-2 reacted species. The slow Si-2 attenuation can be seen to result from the balance between Si-2 attenuation by the overlayer and Si-2 creation by the laterally growing patches.

Decomposition of the core emission demonstrates that the third Si species appears at nominal coverages of 3 ML and all three Si components are present in about equal strength in the surface region for $\theta \approx 5$ ML ($\sim 8\%$ of the original signal). At this coverage, the valence-band results show a metallic Ce overlayer, and the Si-2 attenuation reveals a covering up of the reacted phase. Indeed, the appearance of Si-3 is coincident with the emergence of peak *A* in the valence bands. Its persistence and nearly constant concentration suggests that Si-3 is segregated within an escape depth from the top of the Ce film. At the same time the large energy shift relative to the clean surface and the sharper line shape show that Si atoms are mostly coordinated to Ce atoms and that considerable charge transfer occurs. For coverages greater than 5 ML, this floating Si is the most prevalent species. By 8–10 ML there is effectively no unreacted Si-1 or reacted Si-2 near the surface, consistent with the completion of silicide formation and Ce covering up. Indeed, by this coverage the valence bands are converging on bulk Ce. The almost complete loss of Si-1 and Si-2 signals by 8 ML indicates that the Ce-Si reaction is confined to a thin, well-defined layer. On top of Fig. 2 we schematically show our model of the evolving Ce/Si interface, indicating the lateral growth of the silicide phase, its covering up and the appearance of Si on the Ce overlayer.

Comparison of the present results with other rare-earth/Si interfaces shows similarities and intriguing differences. All the systems studied so far [Ce/Si (Ref. 17), Sm/Si (Ref. 22), Eu/Si (Ref. 23) Yb/Si (Ref. 24)] exhibit a critical coverage for the reaction and large chemical shifts indicative of substantial charge transfer in the reacted phase. On the other hand, while the Ce/Si interface is characterized by a low value of the Schottky barrier, as expected on the basis of recent results for technological samples,¹² no such lowering of the barrier was found for the Sm/Si system.²² This difference is not understood at present and a systematic study of Schottky barrier formation involving rare-earth metals and Si is needed.

Finally, a significant point of this paper has been that high-resolution studies of reactive interfaces make it possible to distinguish the chemical environments of the consti-

tments, i.e., that specific bonding configurations form which can be identified even for intermixed interfaces where long-range order is absent and the scale of the interface is limited to a few monolayers. Hence, we can conclude that strong local bonding determines the character of the evolving interface species. Comparison to bulk compounds will show how the interface phase fits into the hierarchy of the bulk phase diagram. For Ce/Si, we find no evidence that more than a single silicide phase exists, and whatever stoichiometry gradients might exist between the reacted patches and the unreacted Si are too small for identification. By studying the variation of each component with nominal metal overlayer coverage, even complex interfaces can be modeled. The implications of these conclusions are major

because they indicate the limitations of modeling of interface properties based on homogeneous overlayers and they show the importance of microscopic fingerprinting of interface phases.

This work was supported by the Army Research Office under Contract No. ARO-DAAG-29-83-K-0061. The Wisconsin Synchrotron Radiation Center is supported by the National Science Foundation, and the cheerful support of its staff is gratefully acknowledged. Stimulating discussions with S. A. Chambers contributed to this work. Two of us (J.J. and D.G.O.) are also affiliated with Materials Science Program, University of Wisconsin.

- ¹E. H. Rhoderick, *Metal-Semiconductor Contacts* (Clarendon, Oxford, 1978).
- ²For a general overview on metal semiconductor interfaces, see L. J. Brillson, *Surf. Sci. Rep.* **2**, 123 (1982); G. Margaritondo, *Solid-State Electron.* **26**, 499 (1983).
- ³A. Zunger, *Phys. Rev. B* **24**, 4372 (1981).
- ⁴R. R. Daniels, A. D. Katnani, Te-Xiu Zhao, G. Margaritondo, and A. Zunger, *Phys. Rev. Lett.* **49**, 895 (1982).
- ⁵R. Ludeke, T. C. Chiang, and T. M. Miller, *J. Vac. Sci. Technol. B* **1**, 581 (1983).
- ⁶P. Skeath, I. Lindau, C. Y. Su, and W. E. Spicer, *Phys. Rev. B* **28**, 7051 (1983).
- ⁷J. H. Weaver, M. Grioni, and J. Joyce, *Phys. Rev. B* (to be published).
- ⁸P. Oelhafen, J. L. Feeouf, T. S. Kuan, T. N. Jackson, and P. E. Batson, *J. Vac. Sci. Technol. B* **1**, 588 (1983).
- ⁹J. Freeouf and J. M. Woodall, *Appl. Phys. Lett.* **36**, 690 (1981).
- ¹⁰P. McKinley, G. J. Hughes, and R. M. Williams, *J. Phys. C* **15**, 7049 (1982).
- ¹¹L. J. Brillson, *Phys. Rev. B* **18**, 2431 (1978).
- ¹²R. D. Thompson, B. Y. Tsaur, and K. N. Tu, *Appl. Phys. Lett.* **38**, 535 (1981).
- ¹³M. Saitoh, F. Shoji, K. Oura, and T. Hanawa, *Jpn. J. Appl. Phys.* **19**, L421 (1980).
- ¹⁴G. Le Lay and J. P. Faurie, *Surf. Sci.* **69**, 295 (1977).
- ¹⁵F. Ringeisen, J. Derrien, E. Daugy, J. M. Layet, P. Mathiez, and F. Salvan, *J. Vac. Sci. Technol. B* **1**, 546 (1983).
- ¹⁶J. D. McCaldin, *J. Vac. Sci. Technol.* **11**, 990 (1974).
- ¹⁷M. Grioni, J. Joyce, S. A. Chambers, D. G. O'Neill, M. del Giudice, and J. H. Weaver, *Phys. Rev. Lett.* **53**, 2331 (1984).
- ¹⁸G. Margaritondo, J. H. Weaver, and N. G. Stoffel, *J. Phys. E* **12**, 662 (1979).
- ¹⁹D. M. Wieliczka, C. G. Olson, and D. W. Lynch, *Phys. Rev. Lett.* **29**, 3028 (1984); D. M. Wieliczka, J. H. Weaver, D. W. Lynch, and C. G. Olson, *Phys. Rev. B* **26**, 7056 (1982).
- ²⁰F. J. Himpsel, P. Heimann, T.-C. Chiang, and D. E. Eastman, *Phys. Rev. Lett.* **45**, 1112 (1980); S. Brennan, J. Stohr, R. Jaeger, and J. E. Rowe, *ibid.* **45**, 1414 (1980).
- ²¹M. Fink and A. C. Yates, *At. Data* **1**, 385 (1970).
- ²²A. Franciosi, P. Perfetti, A. D. Katnani, J. H. Weaver, and G. Margaritondo, *Phys. Rev. B* **29**, 5611 (1984).
- ²³C. Carbone (private communication).
- ²⁴E. Rossi, J. Nogami, I. Lindau, L. Braicovich, I. Abbati, U. del Pennino, and S. Nannarone, *J. Vac. Sci. Technol. A* **1**, 781 (1983).